http://journal.uir.ac.id/index.php/JGEET

E-ISSN : 2541-5794
P-ISSN :2503-216X

Journal of Geoscience,
Engineering, Environment, and Technology
Vol 10 No 4 2025

RESEARCH ARTICLE

Geology, Structural Control and Hydrothermal Alteration of Porphyry Copper-Gold Deposits, Prospect Berambang, Sekotong District, West Lombok, West Nusa Tenggara, Indonesia

Andi Faesal[1,*], Melinda Dwi Erintina[2]

[1]*Geological Engineering Department, Universitas Muhammadiyah Mataram, 83115 Mataram City, Indonesia*
[2]*Mining Engineering Department, , Universitas Muhammadiyah Mataram, 83115 Mataram City, Indonesia*

*Author Email: andi.esal@gmail.com
Received: Feb 25, 2025; Accepted: Dec 30, 2025.
DOI: 10.25299/jgeet.2025.10.4.21572

Abstract

Berambang, located in the Sekotong district of West Lombok, West Nusa Tenggara, Indonesia, is part of the eastern Sunda Arc, known for world-class gold mines. The area, situated within a province rich in copper-gold deposits such as the Batu Hijau and Hu'u deposits, is still in the early stages of promising exploration. This study aims to identify and understand the geological factors controlling alteration and mineralization in the Berambang deposit, based on geomorphological, stratigraphic, and structural analyses, supported by fieldwork and laboratory investigations, including petrographic analysis and X-ray diffraction (XRD). The stratigraphy of Berambang is divided into four rock units: dacitic volcanic rock, diatreme breccia, diorite intrusion, and alluvium. Geomorphologically, Berambang consists of three landform units: intrusive hills, volcanic hills, and alluvial plains. Hydrothermal alteration in the area is categorized into four types: argillic alteration (kaolinite-illite-smectite), advanced argillic alteration (alunite-andalusite), propylitic alteration (chlorite-calcite-quartz-epidote), and potassic alteration (biotite-silica-magnetite). Notably, potassic alteration, an indicator of porphyry deposits, has been identified, with hydrothermal fluid activity being controlled by two fault systems in Berambang, trending northeast-southwest and northwest-southeast.

Keywords: Porpyry Cu-Au, Berambang, Alteration, Potasic, Hydrothermal Fluid

1. Introduction

Geographically, Lombok Island is bounded by the island of Bali to the west, the Bali Sea to the north, the island of Sumbawa to the east, and the Indian Ocean to the south (Métrich et al., 2017). Geologically, Lombok lies within the Banda Arc, an archipelago formed by young volcanic mountains (Malawani et al., 2022). The geological composition of Lombok consists of Neogene formations, including old volcanic rocks, intrusive rocks, and sedimentary rocks such as marl, mudstone, and limestone (Mutaqin et al., 2021). The old volcanic rocks are primarily composed of augite-porphyritic andesite, and hornblende-augite rich andesite, predominantly found in the southern parts of Lombok and Sumbawa, extending in a west-east direction (Voigt et al., 2022).

Physiographically, Lombok is part of the Nusa Tenggara Volcanic Arc, which forms a segment of the eastern Sunda Arc and the Banda Arc (Kirchenbaur et al., 2022) (Figure 1.a). The stratigraphic sequence of Lombok comprises Neogene rocks (the oldest units) and Quaternary Vulcanic rocks (the youngest units), dominated by volcanic rocks and intrusive rocks (Tang et al., 2024). These rocks date back to the Neogene and Quaternary periods (Mangga et al., 1994).

During the Oligocene, underwater volcanic activity resulted in the deposition of volcanic materials associated with the Pengulung and Kawangan Formations (Persaulian and Noor, 2016). This volcanic activity persisted into the Early Miocene, driven by the subduction of the Indian Ocean Plate beneath the Eurasian Continental Plate (Zhang et al., 2022). In the Middle Miocene, magmatic activity produced dacite and basalt intrusions that penetrated the Pengulung and Kawangan Formations, characterized by post-magmatic processes leading to alteration, ore mineralization, and the development of quartz veins within the intruded rocks (Kirom et al., 2024). In the Late Miocene, the development of basins facilitated the deposition of limestone from the Ekas Formation, marking the transition from the Neogene to the Early Quaternary (Winarti et al., 2016).

Normal faults and strike-slip faults dominate the geological structures of Lombok Island, exhibiting general trends in the northwest-southeast, southwest-northeast, and north-south directions (Sarjan et al., 2021) (Figure 2.b). The oldest tectonic activities in this region are thought to have occurred during the Oligocene, accompanied by underwater volcanic activity characterized by andesite-basalt deposits that formed the Pengulung and Kawangan Formations, producing distinctive volcanic structures and facies such as pillow lavas (Persaulian and Noor, 2016).

During the Late Tertiary to Early Quaternary, fault systems developed with varying orientations, including southwest-northeast, south-southwest to north-northeast, and north-south trends (Supendi et al., 2020). These faults are believed to have remained active from the Tertiary to the Quaternary (Felix et al., 2022). A regional gravity survey confirmed the presence of a fault structure trending north-northeast to south-southwest (Priyono et al., 2021). Additionally, lineament interpretations from Landsat imagery revealed linear features trending south-southwest to north-northeast (Nasution et al., 2010).

One area of geological interest is Berambang, which hosts significant gold mineralization (Idrus et al, 2021). The geological structures controlling this mineralization exhibit general orientations of northeast-southwest and northwest-southeast (Fatimah et al., 2024). Joints and faults in the areaenhance its mineralization potential. Exposed intrusive

rocks along the edges of the Berambang Village road display intersecting veins, forming stockwork structures with abundant ore mineralization (Ubaidillah et al., 2019). These stockworks are the result of hydrothermal fluids filling intersecting fractures, enabling the deposition of ore minerals (Faesal et al., 2022).

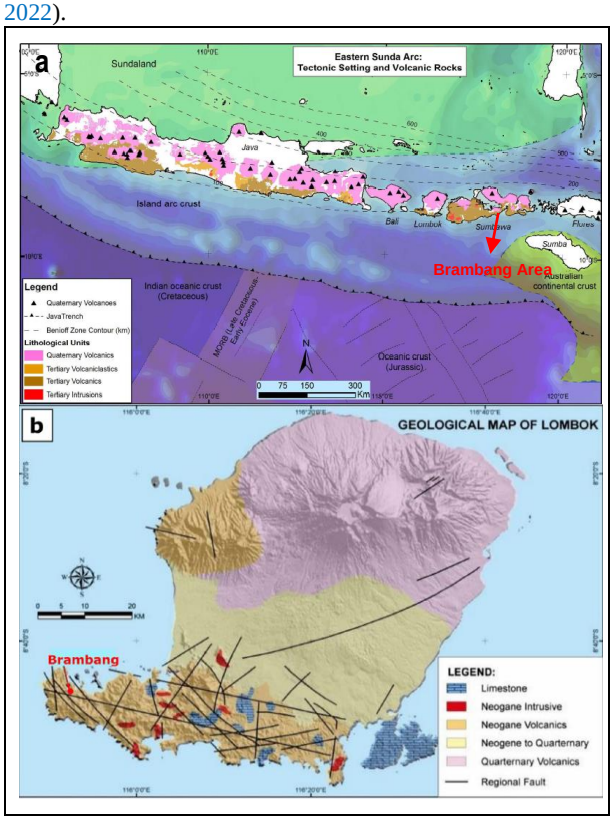

Figure 1. (a) Regional map of the eastern Sunda Arc and the Banda Arc showing the location of the Brambang area (modified from Setijadji & Maryono, 2012), and (b) the geological map of Lombok Island (modified after Faesal et al., 2022).

2. Methodology

The research methodology involved the collection of both primary and secondary data. Secondary data were sourced from books, journals, papers, and relevant agencies, while primary data were obtained through field sampling of surface rocks. Field observations focused on megascopic characteristics, followed by laboratory analyses to refine the findings. Laboratory analyses were conducted at Gadjah Mada University and included petrographic examination of thin sections and X-ray diffraction (XRD) analysis to determine mineralogical and structural compositions. These combined approaches provided a comprehensive framework for understanding the geological characteristics under study, adhering to established analytical standards (Craig and Vaughn, 1994).

3. Results and Discussion

3.1 Geomorfology

The study area comprises three primary landform units: The classification of landform units in the study area follows the geomorphological framework proposed by Zuidam (1983), which integrates three principal components: morphology—comprising morphography and morphometry—and morphogenesis, which includes morphostructure and morphodynamics. This methodological approach enables a comprehensive characterization of landforms and the processes governing their development.

The first landform unit is identified as **Volcanic Hills**. Morphographically, this unit exhibits an elongated hilly topography trending predominantly east–west. Morphometric analysis shows that the hills possess steep slopes ranging from 30% to 70%, with elevation differences between 20 and 270 m above sea level. In terms of morphogenesis, the unit represents a passive morphostructural domain composed of volcanic rocks that have undergone uplift and denudation without recent tectonic reactivation (Figure 2.a). The morphodynamic processes shaping this unit include continual erosion, weathering, and sedimentation. Based on these characteristics, the Volcanic Hills unit occupies approximately 60% of the mapped area and is marked by moderately rugged to steep relief formed over relatively resistant volcanic lithologies (Figure 3).

The second unit is classified as **Intrusive Hills**, which also display a hilly morphology but differ from the volcanic unit due to their intrusive igneous composition. Morphometric parameters indicate slope gradients of 30%–70% and elevations ranging from 20 to 230 m above sea level (Figure 2.b).. The passive morphostructure of this unit is inferred from the contour patterns, which reveal the presence of resistant intrusive bodies. Morphodynamically, the development of these hills is governed by differential weathering and erosion processes acting upon the intrusive lithologies. The Intrusive Hills unit covers approximately 20% of the study area and tends to form prominent topographic highs due to the relatively high resistance of the igneous rocks against erosional forces (Figure 3).

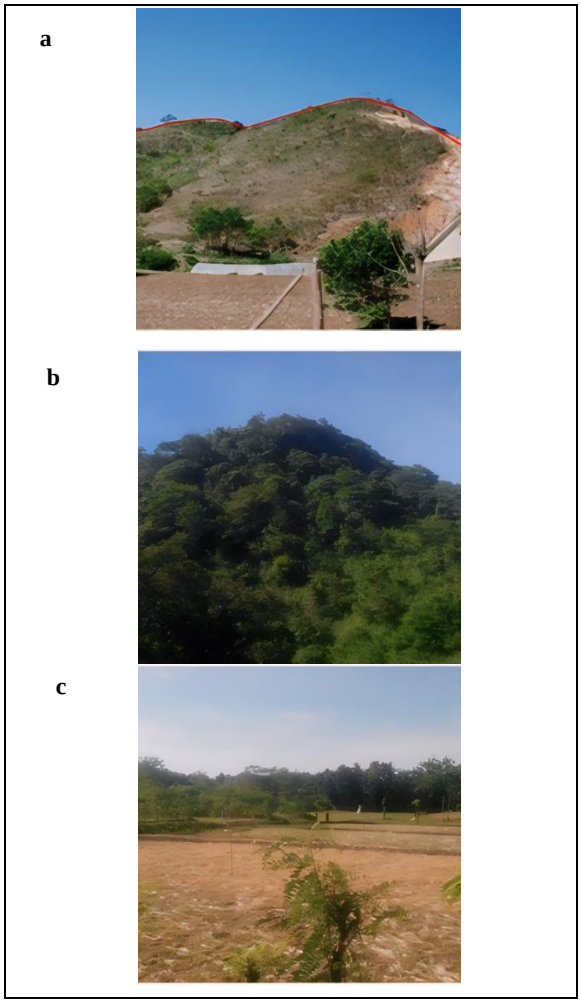

Fig 2. (a) Geomorphology of the vulcanic Hills Landform. (b) Intrusive Hill Landform. (c) alluvial plain Landform

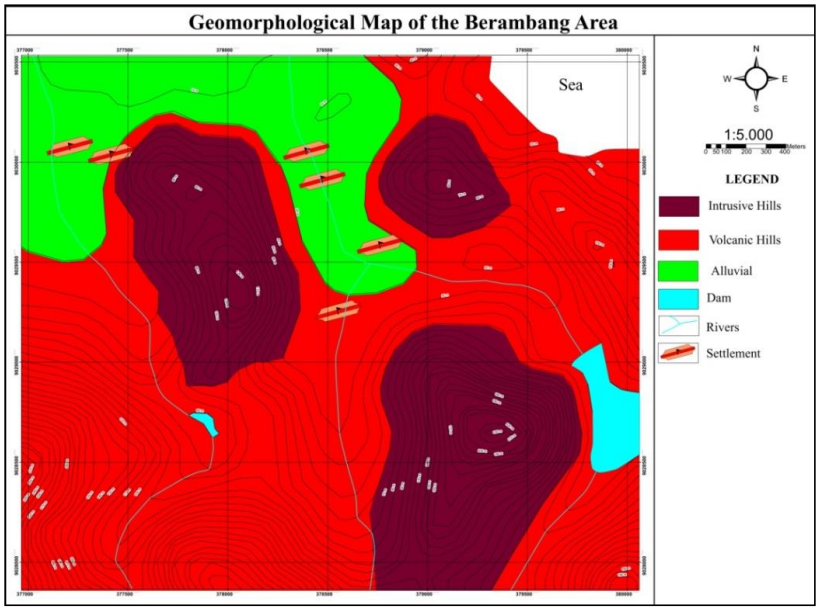

Fig 3. Geomorphological map of the Berambang area depicting the spatial distribution of landform units

The third landform unit corresponds to an **Alluvial Plain**, which is morphographically characterized by a flat surface. Morphometric analysis shows that the plain features very gentle slopes of 0%–2% and elevations between 2 and 15 m above sea level (Figure 2.c). Morphogenetically, this unit represents a passive morphostructural domain composed of unconsolidated materials derived from the mechanical breakdown of source rocks and subsequently transported by fluvial processes (Figure 3). Its morphodynamic behavior is strongly influenced by active erosion, weathering, and deposition, resulting in a low-relief landscape with weak material resistance and a sedimentary fill dominated by fine- to coarse-grained alluvium

Overall, the three landform units reflect geomorphological variability controlled by lithology, structural setting, and active surface processes. The integration of morphographic, morphometric, and morphogenetic data provides a robust basis for delineating geomorphological units and interpreting the landscape evolution within the study area.

3.2 Stratigraphy

The study area comprises two primary lithological units: the dacitic volcanic unit and the diatreme breccia unit, both informally designated due to the limited scope of the study area relative to the larger regional formations. The dacitic volcanic unit occupies 50% of the area and is characterized by extensively altered rocks, where the original texture and mineralogy are unrecognizable (Figure 5).

This unit trends from the southwest to the northeast and exhibits reddish-white coloration, very fine-grained mineral composition (0.05–0.8) mm. Its mineral composition includes quartz (40%) (4C), clay minerals (30%) (3H), opaque minerals (5%) (5F) (Figures 4.a and 4.b). This unit is associated with the Pengulung Formation of Early Miocene age, and its stratigraphic relationship with the overlying river alluvial sedimentary rocks is unc onformable.

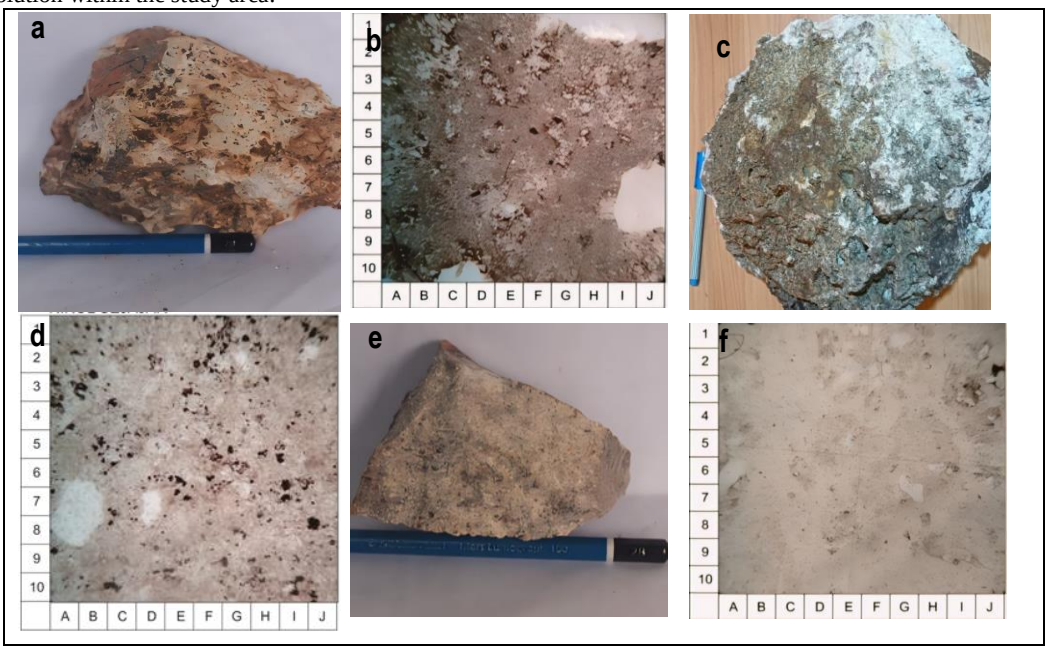

Fig 4. (a) Appearance of an argillic altered dacitic volcanic unit. (b) Presence of clay minerals in microscopic appearance. (c) Appearance of argillic altered megascopic diatreme breccia units, (d) appearance of microscopic diatreme breccia units. (d) Appearance of Diorite intrusion with advanced argillic alteration. (f) Microscopic appearance of the diorite intrusion

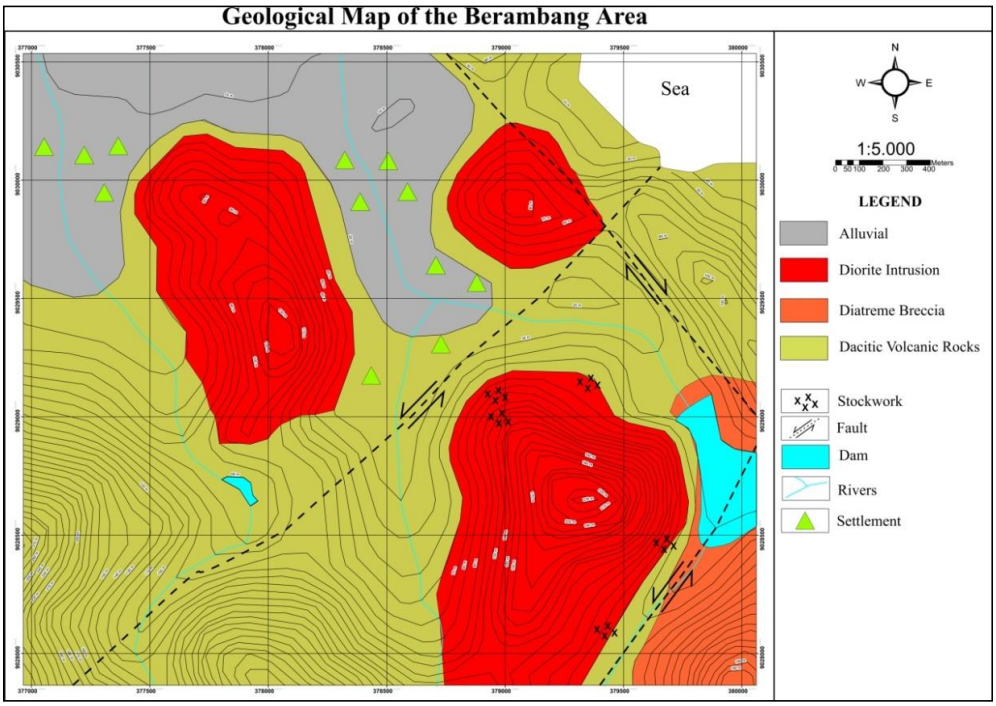

Fig 5. Geological map of the Berambang area illustrating the stratigraphy of the study area

The diatreme breccia unit, also informally designated, represents a smaller part of the Pengulung Formation. This unit formed through magmatic-hydrothermal processes associated with the latest diorite intrusions into the dacitic volcanic unit, controlled by fault structures (Figueroa et al., 2022). The diatreme breccia unit is correlated with the Pengulung Formation of Middle Miocene age. Its stratigraphic relationships include congruence with the underlying dacitic volcanic unit, intrusive contact with the intrusive rocks, and disconformity with the overlying river alluvial deposits. These lithological and structural relationships reflect the complex magmatic and hydrothermal evolution of the area (Figures 4.c. Petrographically, it exhibits reddish-white coloration, partial alteration, grain sizes of 0.2–0.6 mm. The breccia is composed of quartz (60%) (7G), clay minerals (22%) (3D), opaque minerals (3%) (8J), and tuff (15%) (Figures 4.d).

The study area includes the diorite intrusion unit and alluvial deposits, each with distinct lithological and stratigraphic characteristics. The diorite intrusion unit displays variable alteration, predominantly advanced argillic and propylitic. In several areas, the diorite is only weakly to moderately altere (Figure 4.e). Advanced argillic-altered diorite is characterized by a grayish-white color, grain sizes of 0.1–1 mm. Its mineral composition includes alunite (40%) (6G), quartz (43%) (3E), clay minerals (15%) (4H), and opaque minerals (2%) (2J) (Figure 4.f). This unit is correlated with intermediate intrusions of Middle Miocene age. The diorite intrusive unit exhibits intrusive contact with the underlying dacitic volcanic unit and an unconformable relationship with the overlying alluvial deposits (Figure 5).

The alluvial deposits in the study area consist of unconsolidated materials formed through fluvial processes in the Panguluran River. These deposits include fragments of surrounding lithologies, such as lava, breccia, and volcanic materials, with occasional breccia occurrences. The deposits are attributed to Holocene age and reflect the ongoing geomorphological processes in the region. These stratigraphic and lithological relationships highlight the complex geological history and the interplay of magmatic and sedimentary processes in the study area.

3.3 Geological Structure

The Brambang Shear Fault, named after its location near Mount Berambang is characterized by two faults trending northeast-southwest and one fault trending northwest-southeast. The preliminary evidence used as a reference consists of lineament analyses derived from contour maps and DEM imagery, which serve as the basis for interpreting the presence of weak structural zones that have developed within the study area (Figure 6).

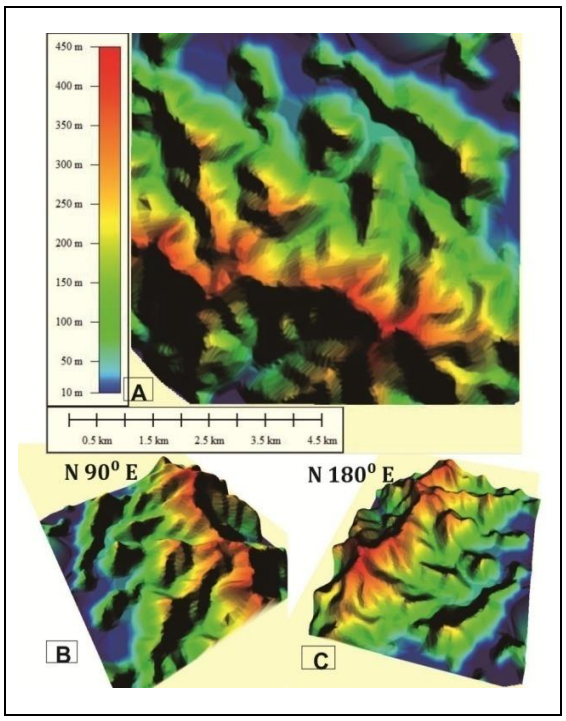

Fig 6. DEM imagery of the Berambang area: (A) a 2-dimensional representation and (B–C) 3-dimensional visualizations generated from contour map configurations produced by the Geospatial Information Agency (BIG)

Field evidence of the Brambang strike-slip fault includes scoured joint structures observed in the dacitic and breccia volcanic rock units at the site (Figure 7.a). These fault structures are associated with fault valleys and escarpments, which are represented by ridges that align with the northwest-southeast and northeast-southwest trends (figure 7.c). The formation of diatreme breccias is linked to these shear faults, which serve as pathways for upwardly migrating hydrothermal fluids (Figure 7.b). The interaction of these fluids with the host rocks facilitates mineralization, potentially resulting in the formation of ore bodies. This geological process highlights the role of fault systems in controlling fluid migration and mineral deposit formation in the region.

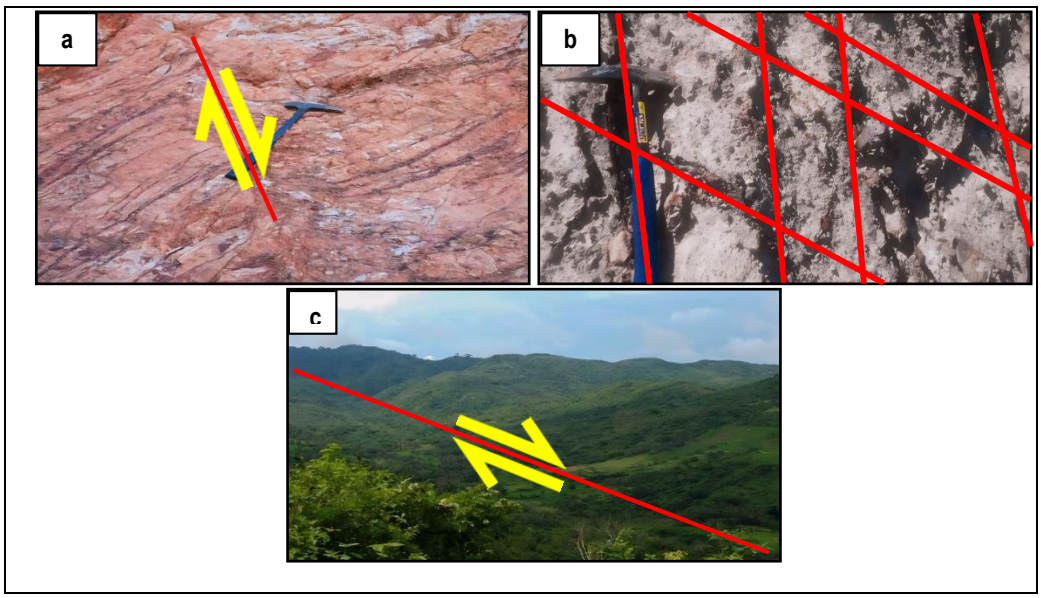

Fig 7. (a) Appearance of a minor fault in the form of a normal fault. (b). The appearance of burrowed joints at the Mount Berambang location indicates a fault. (c) Appearance of the fault scarp taken from Mount Berambang to the northeast. The camera faces northwest

3.3 HydrothermalAlteration

Hydrothermal alteration in the research area is well-defined and predominantly observed in dacitic volcanic rocks, diorite, and diatrema breccias. The alteration zones were identified based on field data interpretations, mineralogical analysis from petrographic studies, and classifications following Corbett and Leach (1997). Argillic alteration is the most extensive, covering approximately 30% of the area in a northeast-southwest orientation (Figure 12). Field observations reveal reddish-white altered rocks, indicative of clay mineral dominance, with alteration zones ranging in thickness from <2 m to 7 m (Figure 8.a).

Microscopic analysis shows a brownish appearance under parallel nicols and gray coloration under cross nicols, with alteration affecting 40%–50% of the rock, replacing most primary minerals selectively to pervasively (Figure 8.b). The identified alteration mineral assemblage consists primarily of clay minerals (20%–37%) (8G) and quartz (50%–69%) (7C) (Figures 8.b). These alterations occur due to interactions between hydrothermal solutions, water, and oxygen near the surface, creating acidic environmental conditions.

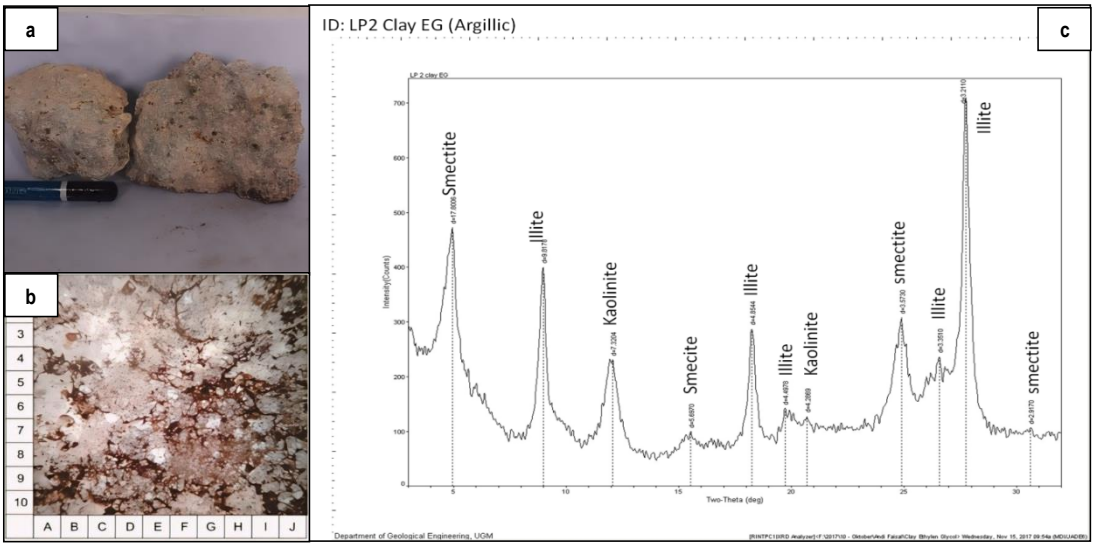

Fig 8. Argillic alteration in rocks. (a) appearance of argillic altered rocks. (b) Photomicrograph of argillic altered rock sample. (c) XRD analysis results for clay minerals in argillic altered rock sample

XRD is employed to precisely identify alteration minerals, including clay minerals and fine-grained secondary phases that are difficult to characterize through petrographic analysis. This technique facilitates the determination of alteration types, the intensity of hydrothermal processes, and the mineralogical characteristics associated with ore-forming systems. Detailed XRD analysis revealed the clay mineral composition, which includes illite, kaolinite, and smectite (Figure 8.c). This mineralogical composition confirms the alteration as argillic, formed at low temperatures (200–250°C) and under low pH conditions (4–5), consistent with the hydrothermal alteration model proposed by Corbett and Leach (1997). These findings highlight the geochemical and mineralogical processes shaping the hydrothermal system in the study area.

Advanced argillic alteration in the study area is distributed across approximately 25% of the total area, trending south to north. This alteration primarily affects dacitic volcanic rocks and diorite, which constitute the wall rocks of the mineralization system (figure 12). Field observations reveal altered outcrops characterized by gray to whitish rocks with visible white clay mineral spots, representing altered plagioclase minerals (Figure 9.a). Petrographic analysis indicates a grayish-white appearance under parallel nicols and a brownish hue under cross nicols, with alteration affecting about 50% of the rock selectively to pervasively, replacing the majority of the original minerals (Figure 9.b).

The alteration mineral assemblage includes clay minerals (10%–20%) (4H), alunite (40%–45%) (6G), and quartz (43%–45%) (4H) (Figure 9.b). Clay minerals are attributed to changes in the groundmass, alunite forms as a product of fluid cooling, and quartz precipitates due to sudden changes in temperature and pressure during hydrothermal fluid cooling. Detailed XRD analysis identified clay minerals such as illite, kaolinite, alunite, anhydrite, and andalusite, as well as smectite (Figure 9.c). The occurrence of illite, kaolinite, and smectite in advanced argillic alteration zones suggests overprinting by argillic alteration.

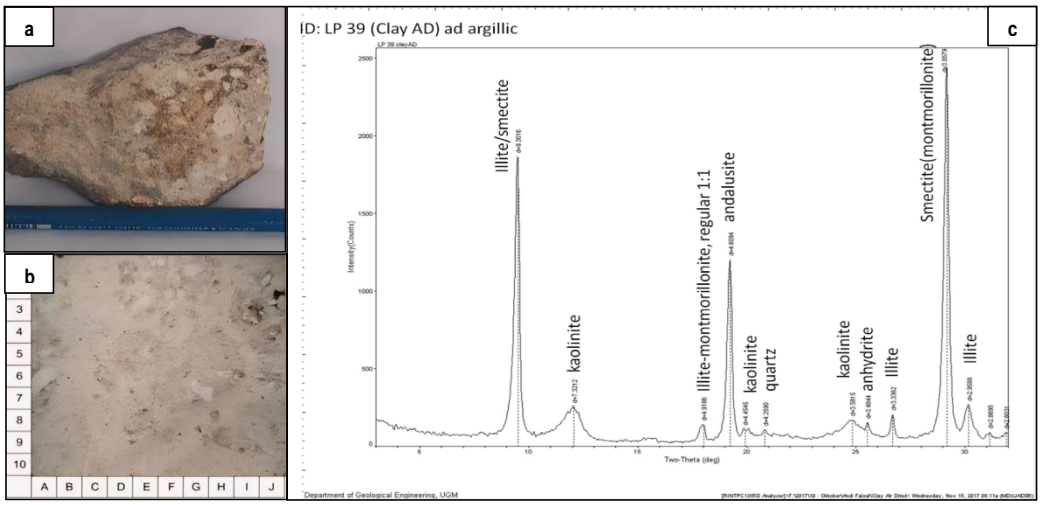

Fig 9. Advanced argillic alteration in diorite rock. (a) Appearance of diorite rock with advanced argillic alteration. (b) Photomicrograph of advanced argillicaltered diorite rock sample. (c) XRD analysis results for clay minerals in advanced argillic altered rock sample

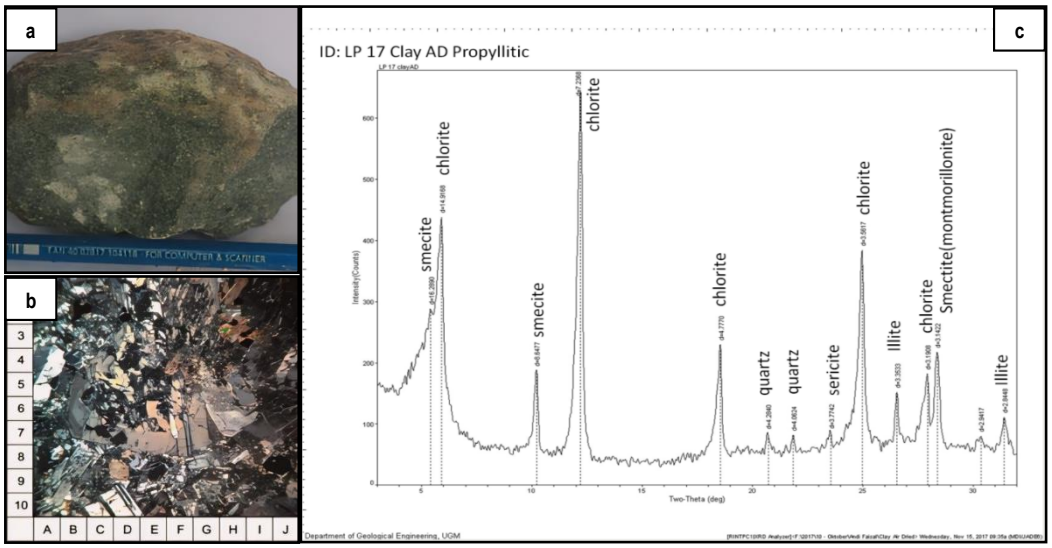

Fig 10. Propylitic alteration rock data. (a) Hand sample of porphylitic altered diorite intrusion. (b) Photomicrograph of propylitic altered rock sample. (c) XRD data for prophylitic altered rock sample.

The advanced argillic alteration is defined by the presence of quartz, alunite, and andalusite, characterizing it as a high-temperature alteration type, typically formed at temperatures of 250–300°C and under low pH conditions (≥4) (Corbett and Leach, 1997). These mineralogical and geochemical characteristics provide insights into the hydrothermal processes and environmental conditions that contributed to the alteration and mineralization in the study area.

Propylitic alteration is present across approximately 20% of the study area, trending southeast to northwest, and primarily affects dioritic rocks (Figure 12). Altered outcrops are characterized by grayish-green rocks, where the original

porphyritic texture with plagioclase phenocrysts remains observable (Figure 10.a). Petrographic analysis reveals brown-green colors under parallel nicols and dark gray colors under crossed nicols, indicating 10%-50% alteration, where the alteration process affects only specific minerals (Figure 10.b).

The primary alteration minerals identified include chlorite (10%-17%) (2I), quartz (25%-40%) (3G), and epidote (3%-8%) (10B), with chlorite and epidote forming from the alteration of Mg/Fe-bearing minerals such as pyroxene, plagioclase, and biotite. Clay minerals such as chlorite, calcite, and epidote were identified in the altered rock samples (Figure 10.c). These minerals are characteristic of propylitic alteration, which is typically associated with low-grade metamorphism of volcanic rocks

Based on the mineral assemblage dominated by chlorite, calcite, quartz, and epidote, this alteration is classified as propylitic, forming at temperatures between 200–250° C and under low pH conditions (≥4), according to Corbett and Leach (1997). These findings highlight the hydrothermal conditions under which the propylitic alteration occurred and provide insights into the geochemical processes at play in the study area.

Potassic alteration is observed in a limited area of the study region, primarily affecting diorite and tonalitec (Figure 12). Altered rocks are characterized by a grayish-green, holocrystalline texture, and exhibit quartz veins filling fractures with multiple intersecting directions (Figure 11.a). Petrographic analysis reveals a greenish-yellowish gray color with an equigranular texture. The dominant minerals include plagioclase (50%) (3I), quartz (20%) (4H), and pyroxene (7%) (5C) which has been altered to actinolite (2%) (5C). Secondary minerals identified include silica (9%) (10D), biotite (4%) (8F), and epidote (3%) (H-I,7—8) (Figure 11.b).

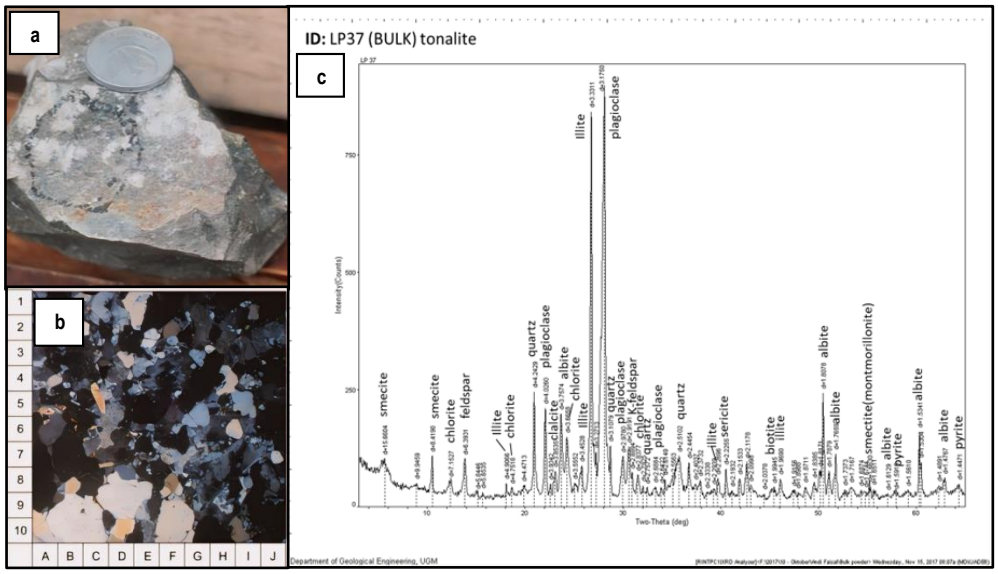

Fig 11. Potassic alteration rock data. (a) Hand sample of potassic altered diorite rock. (b) Photomicrograph showing the potassic altered diorite rock. (c) XRD data of potassic altered diorite rock

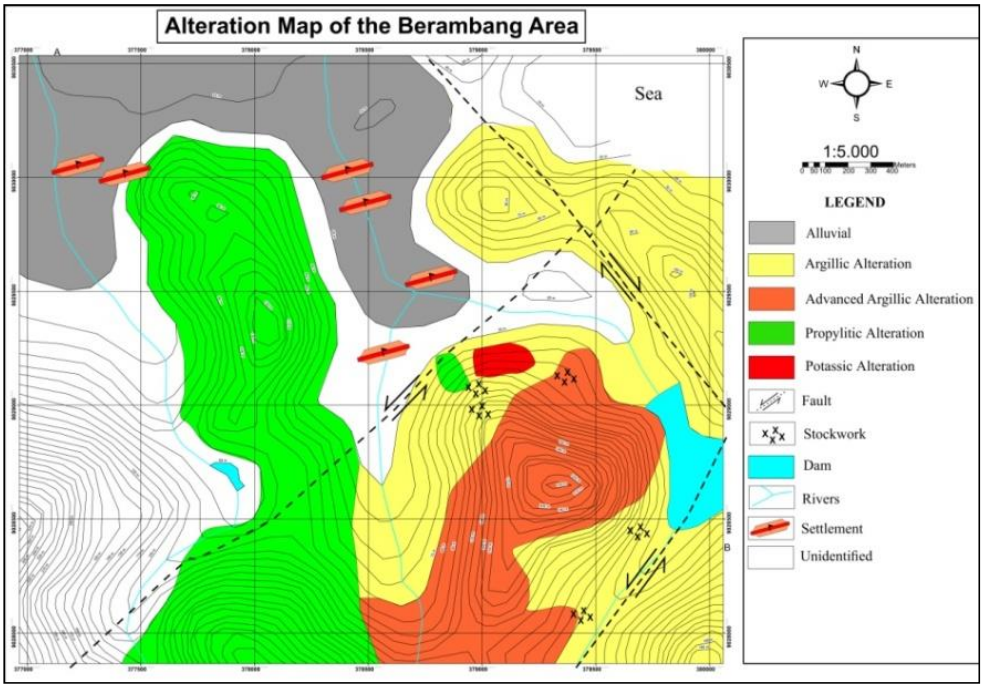

Fig 12.The alteration zoning map of the Berambang area demonstrates the presence of a Cu–Au porphyry-type deposit, indicated by the occurrence of potassic alteration within the study area

Bulk XRD analysis confirms the presence of biotite and K-feldspar, while the clay fraction analysis identifies smectite, chlorite, and illite, suggesting overprinting of potassic alteration with earlier argillic and propylitic alterations (Figure 11.c). The mineral assemblage, including quartz, actinolite, biotite, and magnetite, is characteristic of potassic alteration, which typically forms at temperatures greater than 300°C under high salinity conditions, as described by Corbett and Leach (1997). This alteration type is indicative of hydrothermal processes occurring at high temperatures and salinity, contributing to the geochemical evolution of the area.

4. Discussion

Based on geomorphology, lithology, and geological structures observed in the Brambang area, the region can be classified into two main formations and two landform units. The structural origin formations consist of fault-line escarpment landforms, while the fluvial origin formations include river body forms, with the flow pattern displaying a subparallel configuration. Stratigraphic units in Brambang are informally named based on their lithological characteristics, which can be observed in the field, as well as their stratigraphic position in relation to the overlying and underlying units. The stratigraphic sequence, from oldest to youngest, is as follows: the dacitic volcanic unit, diatrema breccia unit, diorite intrusion unit, and alluvial deposit unit.

Geological structures in Brambang, identifiable through topographic maps, include fault planes and fault scarps. Field observations and fault analysis reveal two primary fault trends in the area: one trending northeast-southwest and the other northwest-southeast.

Alteration processes in Brambang are categorized into four alteration zones based on mineral assemblages: argillic alteration (kaolinite-illite-smectite), advanced argillic alteration (alunite-andalusite), propylitic alteration (chlorite-calcite-quartz-epidote), and potassic alteration (biotite-silica-magnetite). Potassic alteration occurs under temperatures of 300º–390º C and neutral to alkaline pH conditions, with minerals such as biotite, actinolite, and magnetite forming. Propylitic alteration, characterized by chlorite, calcite, and epidote, forms at temperatures between 225º–320º C under neutral to alkaline pH conditions. Advanced argillic alteration, marked by alunite and andalusite, develops at temperatures of 280º–320º C and pH levels of 4–6, while argillic alteration, consisting of kaolinite, illite, and smectite, forms at temperatures of 130º–210º C with a pH range of 4–6. These alteration zones reflect mineralogical transformations driven by variations in temperature and pH within the hydrothermal fluid.

5. Conclusion

The geological characteristics of the Berambang prospect indicate that alteration and mineralization are strongly controlled by lithological variations, structural configurations, and hydrothermal processes associated with Miocene magmatism. The integration of geomorphological, stratigraphic, petrographic, and XRD analyses reveals four dominant alteration types—argillic, advanced argillic, propylitic, and potassic—developing primarily within dacitic volcanic rocks, diatreme breccias, and diorite intrusions. The identification of potassic alteration, together with the presence of quartz stockworks and structurally controlled fluid pathways defined by NE–SW and NW–SE fault trends, suggests a magmatic-hydrothermal system with characteristics consistent with a porphyry Cu–Au environment. These findings demonstrate that the Berambang area hosts a potentially significant mineralization system, with fault-controlled hydrothermal fluid migration playing a critical role in the distribution and intensity of alteration zones, thereby highlighting its promising potential for further exploration and resource evaluation.

Acknowledgements

The author expresses sincere gratitude to the PT Bintang Bulaeng Persada project team for granting permission to conduct the field investigation and for their invaluable assistance throughout the fieldwork at the Brambang Prospect area. The author is also deeply thankful to the lecturers of the Geological Engineering Department and the Diploma Program in Mining Engineering, Universitas Muhammadiyah Mataram, for their continuous academic guidance, constructive discussions, and support during the completion of this research. Their contributions have been fundamental to the successful execution of this study.

References

Corbett, G. J., & Leach, T. M. (1997). Southwest Pacific Rim Gold-Copper Systems: Structure, Alteration, and Mineralization. SEG Special Publication No. 6.

Craig, J.R. and Vaughan, D.J. (1994) Ore Microscopy and Ore Petrography. 2nd Edition, John Wiley & Sons Inc., Hoboken, 424.

Faesal, A., Aminuddin, M.I.K.A., & Ubaidillah, A.S. (2022). Host rock petrology, hydrothermal alteration characteristics & ore mineralogy of porphyry copper-gold deposit, Brambang, Lombok, West Nusa Tenggara Indonesia. Materials Today: Proceedings.

Fatimah, D. Y., Irsyada, M. H., & Nugroho, R. P. (2024). Geological structure control on hydrothermal alteration distribution in Sekotong district, Lombok, Indonesia. AIP Conference Proceedings, 3076, 180001. https://doi.org/10.1063/5.0208942

Felix, R. P., Hubbard, J. A., Bradley, K. E., Lythgoe, K. H., Li, L., & Switzer, A. D. (2022). Tsunami hazard in Lombok and Bali, Indonesia, due to the Flores back-arc thrust. Natural Hazards and Earth System Sciences, 22, 1665–1682. https://doi.org/10.5194/nhess-22-1665-2022

Figueroa, A. J. T., Gabo-Ratio, J. A. S., Manalo, P. C., Takahashi, R., Sato, H., & Aljess. (2022).Breccia and vein mineralization of the Balatoc Diatreme, Acupan gold deposit, Baguio Mineral District: An example of a diatreme-hosted epithermal deposit in the Philippines. Ore Geology Reviews, 144, 104826. https://doi.org/10.1016/j.oregeorev.2022.10482

Idrus, A., Ubaidillah, A. S., Warmada, I. W., & Maula, S. (2021). Geology, rock geochemistry and ore fluid characteristics of the Brambang copper-gold porphyry prospect, Lombok Island, Indonesia. Journal of Geoscience, Engineering, Environment, and Technology, 6(1), 1–12. https://doi.org/10.25299/jgeet.2021.6.1.6145

Kirom, N., Idrus, A., Setijadji, L. D., & Vanessa, A. (2024). Geology and ore mineralization characteristics of the Selodong Prospect, Lombok Island, Indonesia. IOP Conference Series: Earth and Environmental Science, 1373(1), 012038. https://doi.org/10.1088/1755-1315/1373/1/012038

Kirchenbaur, M., Schuth, S., Barth, A. R., Luguet, A., König, S., Idrus, A., Garbe-Schönberg, D., & Münker, C. (2022). Sub-arc mantle enrichment in the Sunda rear-arc inferred from HFSE systematics in high-K lavas from Java. Contributions to Mineralogy and Petrology, 177(8). https://doi.org/10.1007/s00410-021-01871-9

Malawani, M. N., Lavigne, F., Sastrawan, W. J., Jamaluddin, Sirulhaq, A., & Hadmoko, D. S. (2022). The 1257 CE cataclysmic eruption of Samalas volcano (Indonesia) revealed by indigenous written sources. Journal of

Volcanology and Geothermal Research, 432, 107688. https://doi.org/10.1016/j.jvolgeores.2022.107688

Mangga, S. A., Atmawinata, S., Hermanto, B., & Amin, T. C. (1994). Geology of the Lombok Sheet, Nusatenggara, Sheet 1807, Scale 1:250,000. Geological Research and Development Centre.

Métrich, N., Vidal, C. M., Komorowski, J.-C., Pratomo, I., Michel, A., Kartadinata, N., Prambada, O., Rachmat, H., & Surono. (2018). New insights into magma differentiation and storage in Holocene crustal reservoirs of the Lesser Sunda Arc: The Rinjani–Samalas volcanic complex (Lombok, Indonesia). Journal of Petrology, 58(11), 2257–2284. https://doi.org/10.1093/petrology/egy

Mutaqin, B. W., Lavigne, F., Wassmer, P., Trautmann, M., Joyontono, P., Gomez, C., Septiangga, B., Komorowski, J.-C., Sartohadi, J., & Hadmoko, D. S. (2021). Evidence of unknown paleo-tsunami events along the Alas Strait, West Sumbawa, Indonesia. Geosciences, 11(2), 46. https://doi.org/10.3390/geosciences11020046

Naution, A., Takada, T., Udibowo, Widarto, D., & Hutasoit, L. (2010). Rinjani and Propok Volcanics as a Heat Sources of Geothermal Prospects from Eastern Lombok, Indonesia. Jurnal Geoaplika, 5(1), 001–009.

Parsaulian, F. S., & Noor, D. (2016). Geologi dan mineralisasi sulfida daerah Pelangan dan sekitarnya Kecamatan Sekotong, Kabupaten Lombok Barat Nusa Tenggara Barat. Jurnal Online Mahasiswa Teknik Geologi Universitas Pakuan, 1(1).

Priyono, A., Nugraha, A. D., Muzli, M., Ardianto, A., Aulia, A. N., Prabowo, B. S., Zulfakriza, Z., Rosalia, S., Sasmi, A. T., Afif, H., Sahara, D. P., Widiyantoro, S., Wei, S., Husni, Y. M., & Sarjan, A. F. N. (2021). Seismic attenuation tomography from 2018 Lombok earthquakes, Indonesia. Frontiers in Earth Science, 9, 639692. https://doi.org/10.3389/feart.2021.639692

Sarjan, A. F. N., Zulfakriza, Z., Nugraha, A. D., Rosalia, S., Wei, S., Widiyantoro, S., Cummins, P. R., Muzli, M., Sahara, D. P., Puspito, N. T., Priyono, A., & Afif, H. (2021). Delineation of upper crustal structure beneath Lombok using ambient seismic noise tomography. Frontiers in Earth Science, 9, 560428. https://doi.org/10.3389/feart.2021.560428

Setijadji, L. D., & Maryono, A. (2012). Geology and Arc Magmatism of the Eastern Sunda Arc, Indonesia. Proceedings of Banda and Eastern Sunda Arcs, MGEI Annual Convention, 26–27 November 2012.

Supendi, P., Nugraha, A. D., Widiyantoro, S., Pesicek, J. D., Thurber, C. H., Abdullah, C. I., Daryono, D., Wiyono, S. H., Shiddiqi, H. A., & Rosalia, S. (2020). Relocated aftershocks and seismicity in eastern Indonesia. Geophysical Journal International, 221(3), 1845–1855. https://doi.org/10.1093/gji/ggaa118

Tang, G.-R., Dan, W., Maulana, A., Wang, J., Zhang, X.-Z., Zhang, Y.-Y., Ma, X., Wang, Q., Liu, X.-J., & Tang, G.-J. (2024). Arc building and maturation of Lombok Island, East Sunda Arc. Chemical Geology, 663, 122265. https://doi.org/10.1016/j.chemgeo.2024.122265

Ubaidillah, A. S., Idrus, A., Warmada, I., & Maula, S. (2019). Geokimia pada endapan Cu-Au porfiri Brambang, Pulau Lombok. Jurnal Geosapta, 5(2), 103–112. https://doi.org/10.20527/jg.v5i2.5536

Van Bemmelen, R. W. (1949). The Geology of Indonesia, Vol. 1A. Government Printing Office.

Voigt, A., Cassidy, M., Castro, J. M., Pyle, D. M., Mather, T. A., Helo, C., Abdurrachman, M., & Kurniawan, I. A. (2022). Experimental investigation of trachydacite magma storage prior to the 1257 eruption of Mt Samalas. Journal of Petrology, 63(8), egac066. https://doi.org/10.1093/petrology/egac066

Winarti, D., Karnawati, D., Hardiyatmo, H. C., & Srijono. (2016). Mineralogical and geochemical control of altered andesitic tuff at Pelangan, Lombok. Journal of Applied Geology, 1(1), 19–28. https://doi.org/10.22146/jag.26953

Zhang, X., Huang, T.-N., Chung, S.-L., Maulana, A., Mawaleda, M., Tien, C.-Y., Lee, H.-Y., & Liu, P.-P. (2022). Late Eocene subduction initiation in the North Sulawesi Arc, Indonesia. Lithos, 422–423, 106742. https://doi.org/10.1016/j.lithos.2022.106742

Zuidam, R. A. van. (1983). Guide to Geomorphological Aerial Photographic Interpretation and Mapping. ITC, Enschede.